Metallofullerene nanoparticles circumvent tumor resistance to cisplatin by reactivating endocytosis

Xing-Jie Liang[a,1,2], Huan Meng[b,1,3], Yingze Wang[a], Haiyong He[a], Jie Meng[a,b], Juan Lu[a], Paul C. Wang[c], Yuliang Zhao[b,2], Xueyun Gao[b], Baoyun Sun[b], Chunying Chen[a], Genmei Xing[b], Dingwu Shen[d], Michael M. Gottesman[d], Yan Wu[a], Jun-jie Yin[e], and Lee Jia[f]

[a]Chinese Academy of Sciences Key Laboratory for Biomedical Effects of Nanomaterials and Nanosafety, National Center for Nanoscience and Technology of China, Beijing 100190, China; [b]Chinese Academy of Sciences Key Laboratory for Biomedical Effects of Nanomaterials and Nanosafety, Institute of High Energy Physics, Chinese Academy of Sciences, Beijing 100049, China; [c]Laboratory of Molecular Imaging, Department of Radiology, Howard University, Washington, DC 20060; [d]Laboratory of Cell Biology, National Cancer Institute, National Institutes of Health, Bethesda, MD 20892; [e]Center for Food Safety and Applied Nutrition, Food and Drug Administration, College Park, MD 20740; and [f]Developmental Therapeutics Program, Division of Cancer Treatment and Diagnosis, National Cancer Institute, National Institutes of Health, Bethesda, MD 20892

Cisplatin is a chemotherapeutic drug commonly used in clinics. However, acquired resistance confines its application in chemotherapeutics. To overcome the acquired resistance to cisplatin, it is reasoned, based on our previous findings of mediation of cellular responses by [Gd@C$_{82}$(OH)$_{22}$]$_n$ nanoparticles, that [Gd@C$_{82}$(OH)$_{22}$]$_n$ may reverse tumor resistance to cisplatin by reactivating the impaired endocytosis of cisplatin-resistant human prostate cancer (CP-r) cells. Here we report that exposure of the CP-r PC-3-luc cells to cisplatin in the presence of nontoxic [Gd@C$_{82}$(OH)$_{22}$]$_n$ not only decreased the number of surviving CP-r cells but also inhibited growth of the CP-r tumors in athymic nude mice as measured by both optical and MRI. Labeling the CP-r PC-3 cells with transferrin, an endocytotic marker, demonstrated that pretreatment of the CP-r PC-3-luc cells with [Gd@C$_{82}$(OH)$_{22}$]$_n$ enhanced intracellular accumulation of cisplatin and formation of cisplatin-DNA adducts by restoring the defective endocytosis of the CP-r cancer cells. The results suggest that [Gd@C$_{82}$(OH)$_{22}$]$_n$ nanoparticles overcome tumor resistance to cisplatin by increasing its intracellular accumulation through the mechanism of restoring defective endocytosis. The technology can be extended to other challenges related to multidrug resistance often found in cancer treatments.

drug resistance | nanomedicine | nanoimaging | chemotherapy | nanopharmaceutical

As a major chemotherapeutic agent for tumor treatment, cisplatin remains a cornerstone of the present-day chemotherapy regimens against not only epithelial malignancies but also a number of metastatic and advanced malignancies (1, 2). However, because of high toxicity and easy development of drug resistance, successful treatment with cisplatin often is limited (3, 4). Following the discovery of ATP-binding cassette (ABC) transporters and their roles in drug resistance in various types of tumors (5), much research has been done to explore the relationship between ABC transporter activity and specific chemotherapeutics, including cisplatin. Because no ABC transporter has been identified for "pumping" cisplatin out of cisplatin-resistant human prostate cancer (CP-r) cells (6–8), it would be difficult to sensitize CP-r cells by using any known strategy that targets resistant cancer cells by inhibiting multidrug resistance (MDR)–associated proteins on plasma membrane of the CP-r cells. Diffusion has been considered as a pathway for cisplatin to penetrate plasma membrane. Recently, studies have indicated that cisplatin entered cells by endocytosis and other mechanisms (9–12).

To increase susceptibility of cancer cells to cisplatin, i.e., to reverse drug resistance, many efforts have been made through chemical modification, gene therapy, vector delivery, and other means (2, 9, 13). Combination of traditional chemotherapy with nanotechnology may provide a promising alternative for novel cancer treatments. The use of nanoparticles to sensitize tumor cells to cisplatin in vitro and in vivo has been described recently

(14–16). In these studies, cisplatin-encapsulated nanoparticles were used to control release of cisplatin into the CP-r cells (15), and the effects were cell-line specific (16). Nanoparticles have potential for a wide range of biomedical and biotechnological applications. Fullerene molecules, the third form of pure carbon in addition to the diamond and graphite forms, have attracted much attention to their biomedical applications (17). It has been demonstrated that fullerenes can generate singlet oxygen and suppress tumor growth without damage to normal skin of the mice exposed to visible light (18). We have found that metallofullerene nanoparticles penetrate plasma membrane of tumor cells and result, to some degree, in shrinkage of solid tumors in vivo (19, 20). As a proof of concept, we have demonstrated that the metallofullerene nanoparticles, formulated as [Gd@C$_{82}$(OH)$_{22}$]$_n$, are able to effectively inhibit proliferation of solid tumors and to decrease the activities of those enzymes responsible for catalyzing the production of reactive oxygen species in vivo (20–22). In addition, [Gd@C$_{82}$(OH)$_{22}$]$_n$ nanoparticles did not show significant side effects in vivo. In the present study, we showed that multihydroxylated metallofullerene nanoparticles ([Gd@C$_{82}$(OH)$_{22}$]$_n$) could reactivate the defective endocytosis of cisplatin in the CP-r cells and cause accumulation of intracellular cisplatin in the CP-r cells. Consequently, tumor resistance to cisplatin was circumvented by treatment with a combination of [Gd@C$_{82}$(OH)$_{22}$]$_n$ with cisplatin both in vitro and in vivo.

Results and Discussion

Physical Properties and Characterization of [Gd@C$_{82}$ (OH)$_{22}$]$_n$ nanoparticles. Metallofullerenes with gadolinium (Gd) have been demonstrated to be capable of effectively enhancing magnetic resonance image contrast (23). [Gd@C$_{82}$ (OH)$_{22}$]$_n$, synthesized by our group, has been verified as a new generation of highly efficient contrast agents for magnetic resonance imaging (MRI) (24–27). It is a hydroxylated fullerene forming a cage encapsulating gadolinium inside (Fig. S1). The multihydroxylated amphiphilic metallofullerene [Gd@C$_{82}$(OH)$_{22}$]$_n$ self-assembles in aqueous solution to form nanoparticles. These nanoparticles do

MEDICAL SCIENCES

CHEMISTRY

www.manaraa.com

not exist as individual molecules or molecular ions but as aggregates. The average size of $[Gd@C_{82}(OH)_{22}]_n$ aggregates is 50 ± 12 nm, measured by dynamic light scattering (DSL). The particles form nonuniform quasi-spherical shapes. The $[Gd@C_{82}(OH)_{22}]_n$ nanoparticles self-assemble into a hexagonal microstructures that are visible by scanning electron microscopy (Fig. 1 *A* and *B*). This multihydroxylated metallofullerene does not show significant in vivo toxicity as evidenced by morphological analysis of HE staining various tissues of tumor-bearing animals (Fig. 1*C*). Protonation or deprotonation of $[Gd@C_{82}(OH)_{22}]_n$ varies the negative charges of the hydroxyl groups, which further modulates the repulsive static electric forces among the $[Gd@C_{82}(OH)_{22}]_n$ species (28). These repulsive static-electric forces could affect the size of hydrophobic-force–induced self-assembly of $[Gd@C_{82}(OH)_{22}]_n$ nanoparticles. The size determines the nanoparticle-mediated cellular response, and particle size at 40–60 nm appears to have the greatest effects (29).

Development of PC-3 luc Cells Resistant to Cisplatin. In this study, we proposed that $[Gd@C_{82}(OH)_{22}]_n$ nanoparticles reverse tumor resistance by enhancing the endocytosis of cisplatin via nanoparticle-mediated penetration through the plasma membrane of the CP-r cells. To test this hypothesis in vivo and in vitro, human prostate cancer PC-3-luc cells were chosen to establish cisplatin-resistant (CP-r) cells. Luciferase expressed in PC-3 cells was used as a marker to facilitate optical imaging of the CP-r cells. We found that the CP-r PC-3-luc colonies appeared at a frequency of $\approx 1/10^6$ in the presence of cisplatin. The CP-r variants were identified, isolated, and cloned after the parental cisplatin-sensitive (CP-s) cells were exposed to 1 μg/mL cisplatin for 2 months (Fig. S2). To measure cytotoxicity, we cultured the resistant cells in cisplatin-free medium for 10 days before conducting the cisplatin cytotoxicity assay. The resistant index (RI) of the CP-r cells was found to be 6-fold higher than that of the parental CP-s cells (Fig. 2*A*).

$[Gd@C_{82}(OH)_{22}]_n$ Sensitized CP-r Cells to Cisplatin Treatment in Vitro and in Vivo. The CP-r cells were treated with various concentrations of $[Gd@C_{82}(OH)_{22}]_n$ nanoparticles (1–50 μM) with or without 1 μg/mL cisplatin (Fig. 2*B*). The IC$_{50}$ value of cisplatin against parental CP-s cells was 1 μg/mL, the concentration that was used for inducing the CP-r variants and was virtually nontoxic to the CP-r cells. Treatment with $[Gd@C_{82}(OH)_{22}]_n$ nanoparticles alone had no significant effect on either CP-s or CP-r cells at concentrations lower than 10 μM (Fig. S2). Treatment with nanoparticles alone did not change proliferation of the CP-r PC-3-luc cells, nor did cisplatin at 1 μg/mL dosage. However, the number of surviving CP-r cells decreased by ~30% after a combined treatment of 1 μg/mL cisplatin and $[Gd@C_{82}(OH)_{22}]_n$ nanoparticles compared with the nanoparticle or cisplatin treatment alone (Fig. 2*B*). To further confirm the ability of nanoparticles to overcome cisplatin resistance in vivo, we developed a solid tumor mouse model by s.c. injection of 1×10^7 cells in 100 μL sterile saline into the left flank (CP-r PC-3-luc cells) and right flank (CP-s PC-3-luc cells) of athymic nude mice (male, 8–10 weeks old), respectively. Fourteen days after injection, CP-s and CP-r PC-3-luc cells grew into solid tumors having similar sizes. The fluorescence intensities of these tumors were measured by optical imaging. The mice were randomly divided into four groups ($n = 5$ per group) with different treatments for 4 weeks: (*i*) i.p. injection of 1.0 μmol/kg $[Gd@C_{82}(OH)_{22}]_n$ nanoparticles daily (NP group); (*ii*) i.p. injection of 10 mg/kg cisplatin two times per
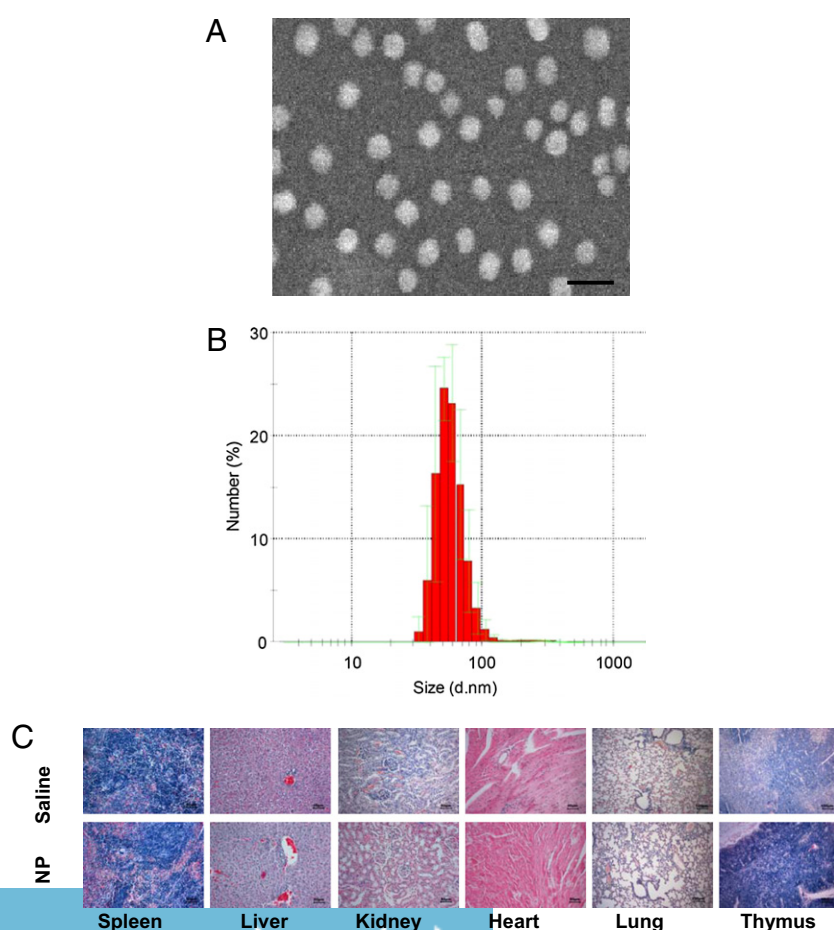

Fig. 1. Characterization of $[Gd@C_{82}(OH)_{22}]_n$ nanoparticles. (*A*) $[Gd@C_{82}(OH)_{22}]_n$ nanoparticles characterized by scanning electron microscopy (SEM). (Scale bar, 100 nm.) (*B*) Size of $[Gd@C_{82}(OH)_{22}]_n$ nanoparticles, as measured by dynamic light scattering (DSL). (*C*) Representative histological H&E staining of various organ tissues from mice treated with $[Gd@C_{82}(OH)_{22}]_n$ nanoparticles or saline. (Scale bar, 50 μm.)

Liang et al.

week (cisplatin group), the same administration schedule used for treatment of cancer patients (to allow comparison across groups, on the day when cisplatin was not injected, 0.15 mL sterile saline was injected into each mouse); (*iii*) i.p. injection of both cisplatin (10 mg/kg, 2 times per week) and $[Gd@C_{82}(OH)_{22}]_n$ nanoparticles (1.0 μmol/kg, daily) (cisplatin+NP); and (*iv*) i.p. injection of saline solution alone (0.15 mL, daily). All mice were weighed daily. Tumor weight was calculated by caliper measurement and tumor volume was determined by MRI analysis (Fig. 2*C*). The

results indicated that $[Gd@C_{82}(OH)_{22}]_n$ nanoparticles improved the inhibition of CP-r tumors growth by cisplatin.

As luciferase is expressed in both the CP-s and CP-r PC-3-luc cells, these prostate cancer cells growing as s.c. tumors on the flanks of the mice can be readily optically imaged in vivo. Representative images of the mice following the 4-week treatment protocol confirmed similarities in CP-s and CP-r tumor proliferation between groups treated with saline or NP. Cisplatin alone was highly efficient at inhibiting CP-s PC-3-luc tumors in vivo but had virtually no effect on the growth of CP-r PC-3-luc tumors in vivo. In contrast, cisplatin combined with the nanoparticles (cisplatin+NP group) inhibited growth of both the cisplatin-sensitive PC-3-luc tumors (as expected) and the cisplatin-resistant PC-3-luc tumors. The sizes of the CP-s PC-3-luc and CP-r PC-3-luc tumors after the combined treatment were very similar (Fig. 2*C* and Fig. 3*A*). MRI images also showed reduced sizes of
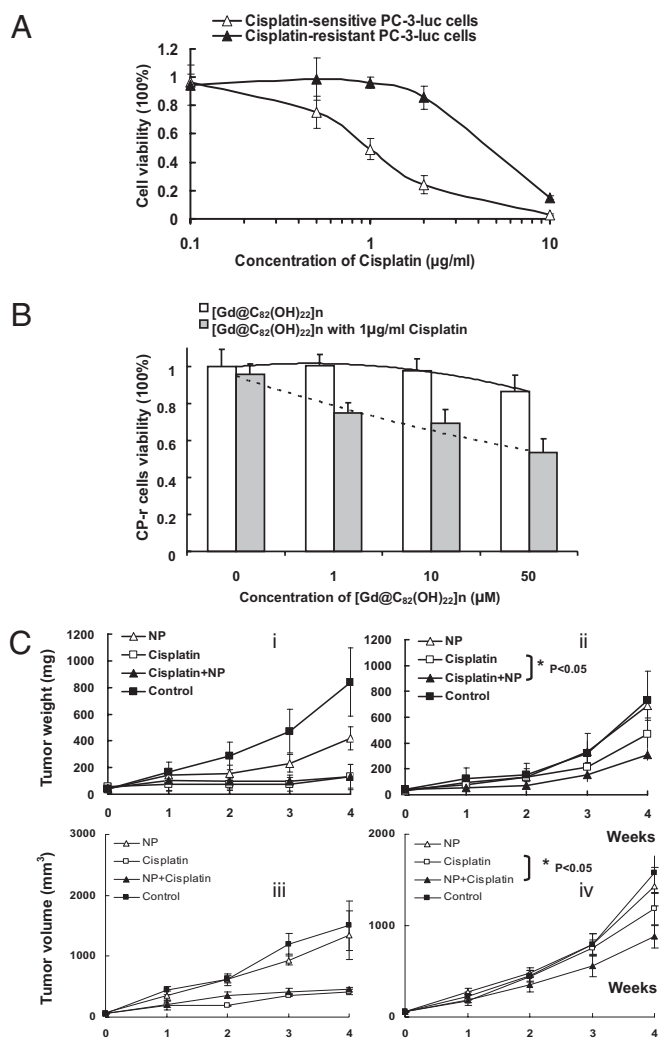

Fig. 2. $[Gd@C_{82}(OH)_{22}]_n$ nanoparticles induced sensitivity enhancement of CP-r cells and tumors to cisplatin. (*A*) Cellular viability curves of CP-s and CP-r PC-3-luc cells treated with cisplatin. Cells (3×10^3) were plated in 96-well plates with 100 μL medium per well. After 6 h, various concentrations of cisplatin in 50 μL medium were added, and the cells were incubated at 37 °C for 3 days. Before the cell viability measurement, 10 μL of MTT solution (Kumamoto) was added to each well and incubated for 2 h. Cell viability was measured using spectrophotometry. (*B*) Measurement of $[Gd@C_{82}(OH)_{22}]_n$ nanoparticle cytotoxicity in CP-r cells treated or untreated with cisplatin (1 μg/mL). The protocol was the same as described in Fig. 2*A*. Results shown are the average of three different experiments. (*C*) Tumor weight was measured by caliper quantification {tumor weight (mg) = tumor density (1 mg/mm^3) × length (mm) × [width (mm)^2 / 2]} (*i*, CP-s PC-3-luc; *ii*, CP-r PC-3-luc). Nanoparticles (20 μM) were used. Tumor volumes were derived from consecutive multiple MRI images using Image J software (*iii*, CP-s PC-3-luc; *iv*, CP-r PC-3-luc). Statistical analysis of *Inset C* using ANOVA shows a significant difference between two sets of data when $P < 0.05$.
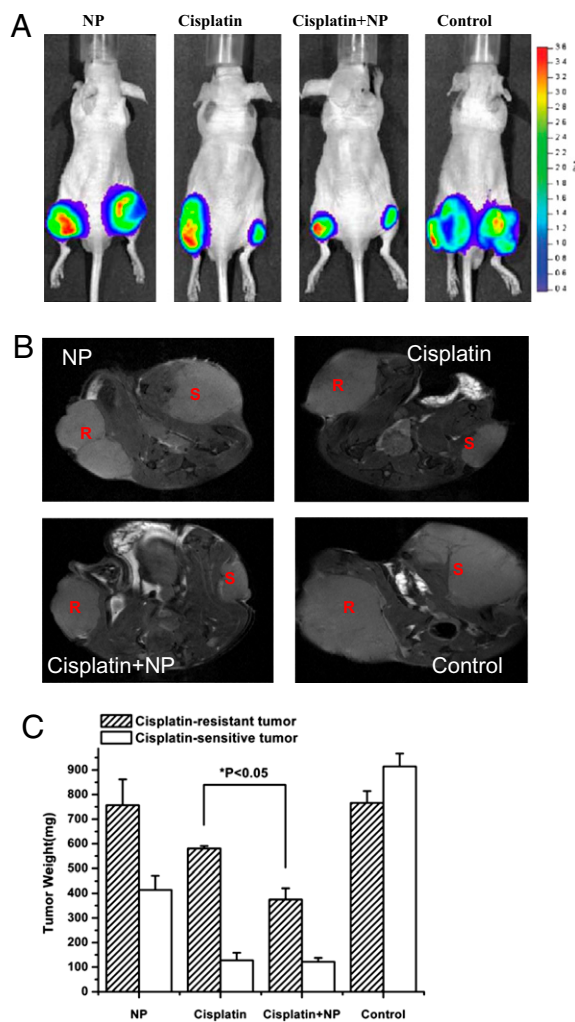

Fig. 3. Sensitizing CP-r tumors to cisplatin treatment by $[Gd@C_{82}(OH)_{22}]_n$ nanoparticles in vivo. (*A*) Optical imaging for comparison of the sizes of CP-s and CP-r PC-3-luc tumors treated with either $[Gd@C_{82}(OH)_{22}]_n$ nanoparticles (NP, 20 μM), cisplatin, cisplatin plus nanoparticles (cisplatin + NP), or saline solution alone as a control. (*B*) MRI images of CP-s and CP-r PC-3-luc tumors after 4 weeks of various treatments described in *A*. (*Right*) CP-s tumor. (*Left*) CP-r tumor. (*C*) Weights of tumors were measured at the end of 4 weeks' treatment. MRI images were analyzed by Image J software for tumor volume. Tumor weight was calculated by conversion of volume to weight. NP (20 μM) treatment significantly enhanced the ability of cisplatin to inhibit growth of CP-r tumors.

Liang et al.

MEDICAL SCIENCES

CHEMISTRY

www.manaraa.com

CP-r and CP-s tumors following the cisplatin plus nanoparticle treatment. A series of multislice MRI images were used to study tumor morphology (shape and location) (Fig. 3B). The tumor volume was calculated based on these consecutive MRI images,

Fig. 4. $[Gd@C_{82}(OH)_{22}]_n$ nanoparticles increased transferrin-mediated endocytosis. Texas Red–transferrin conjugates were used to label CP-s and CP-r PC-3-luc cells for endocytotic measurement. Cisplatin concentration was 1 μg/mL, and $[Gd@C_{82}(OH)_{22}]_n$ was 20 μM. (A–E) Confocal microscopy images. (A) CP-s cells. (B) CP-r cells. (C) CP-r cells treated with cisplatin. (D) CP-r cells treated with nanoparticles. (E) CP-r cells treated with cisplatin and nanoparticles. (F) ICP-MS/MS measurements of DNA adducts in CP-s treated cisplatin; CP-r cells treated with cisplatin with/without $[Gd@C_{82}(OH)_{22}]n$. Data presented are the integrated ICP-MS signals as mean values of yield measurements for various DNA adducts measured by ICP-MS in cells after various treatments. (G) CP-s and CP-r cells were labeled with Texas Red–transferrin for endocytotic measurement. Fluorescence intensity of internalized Texas Red–transferrin was measured by spectrophotometer at an excitation wavelength of 595 nm and emission wavelength of 620 nm. Results shown are mean of three different experiments. Comparisons between groups were evaluated by one-way ANOVA. There was a statistically significant difference between the CP-R cells and CP-R cells treated with nanoparticles.

after which the tumor weight was also statistically calculated and deduced (Fig. 3C). The effect of the nanoparticles on cisplatin treatment was clearly demonstrated in Fig. 3 A and B and as shown by the images of the individual groups (Fig. S3). These studies confirmed that $[Gd@C_{82}(OH)_{22}]_n$ nanoparticles increased the sensitivity of CP-r PC-3-luc tumors to cisplatin in vivo.
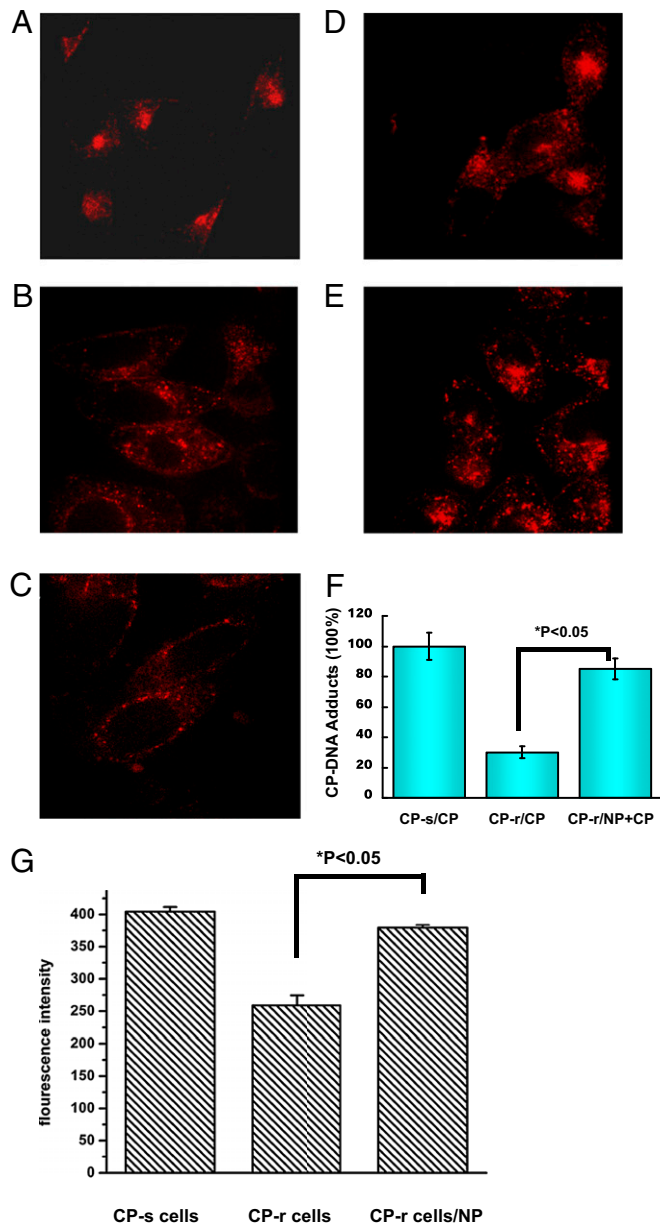
Intracellular Cisplatin Accumulation by Reactivating the Defective Endocytosis in CP-r Cells. Nanoparticles have been used to deliver drugs or genes for cancer treatment using the unique characteristics associated with the nanoscale size (30, 31). It is known that tumors become resistant to cisplatin, partially because of reduced uptake of cisplatin resulting from an endocytic defect following defective formation of the endocytic recycling compartment (ERC) (32). Although the specific molecular or regulatory defect responsible for the reduced accumulation of cisplatin in the CP-r cells has not been identified, several proteins have been found to be associated with this phenotype (33, 34). To investigate how metallofullerene $[Gd@C_{82}(OH)_{22}]_n$ nanoparticles increase cisplatin toxicity in the CP-r cancer cells, the CP-s and CP-r PC-3-luc cells were labeled with Texas Red–transferrin, a bona fide marker of the endocytic recycling pathway. In the parental CP-s PC-3-luc cells, we observed that transferrin localized close to the nucleus as a bright patch of fluorescence. Unlike the pattern observed in the CP-s cells, transferrin was distributed more peripherally in the CP-r cells as discrete punctate structures. In general, there was less intracellular transferrin in CP-r cells compared with CP-s cells (Fig.
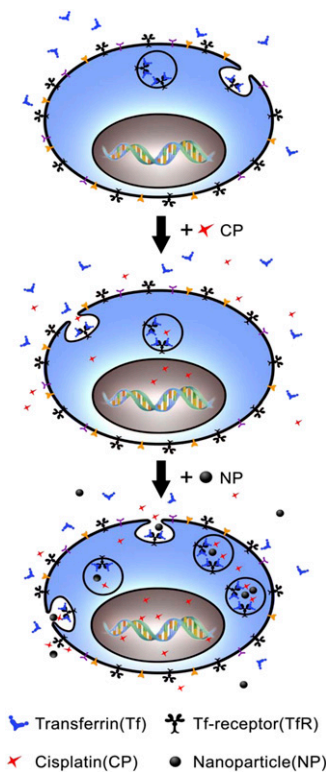

Fig. 5. $[Gd@C_{82}(OH)_{22}]_n$ nanoparticles enhance CP-r cell sensitivity to cisplatin. (Top) Normal endocytosis that includes binding of ligands (e.g., transferrin: Tf) to their Tf-receptors on plasma membrane followed by binding, ingestion into cytoplasma, intracellular vesicle transportation, payload release, and vesicle recycle. (Middle) Receptor-mediated endocytosis of cisplatin in the CP-r cells. Because of defective endocytosis, there is less intracellular accumulation of cisplatin and therefore less formation of cisplatin-DNA adducts in the CP-r cells. (Bottom) Nanoparticle-activated endocytosis in the CP-r cells, resulting in more efficient transportation of cisplatin-containing vesicles and more cisplatin binding to nucleic acid to sensitize the CP-r cells.

4). The difference in transferrin distribution between the CP-r and CP-s cells may result from defective endocytosis of the CP-r cells as demonstrated by our previous studies (32, 35). Cisplatin passes through the plasma membrane and enters cells in part by endocytosis (36–38). We believe that multihydroxylated metallofullerene $[Gd@C_{82}(OH)_{22}]_n$ nanoparticles reactivate endocytosis through their unique nanoscale properties. The reasoning was confirmed by increased nanoparticle-mediated endocytosis in CP-r cells compared with CP-r cells treated with cisplatin alone (Fig. 4 A–E and G). This was also confirmed by increased cisplatin adducts in NP+CP–treated CP-r cells measured using inductively coupled plasma mass spectroscopy (ICP-MS) in the negative ion mode (Fig. 4F). Inhibition of endocytosis by cytochalasin D of Bafilomysin A1 decreased the nanoparticle-activated cisplatin intracellular accumulation (Figs. S4 and S5). This suggests that $[Gd@C_{82}(OH)_{22}]_n$ nanoparticles restore endocytotic function and increase intracellular cisplatin accumulation in CP-r PC-3-luc variants.

Summary. Cisplatin is commonly used to treat prostate cancer at early clinical stages. However, the ability of prostate cancer cells to become resistant to cisplatin remains a significant impediment to successful chemotherapy of prostate cancer patients. It is known that cisplatin enters cells by different pathways such as passive diffusion (39, 40), transportation (41, 42), and endocytosis (14–16), which may be cell-line dependent. Until now, the generally accepted mechanisms by which cells become resistant to cisplatin have been (*i*) enhanced repair ability and tolerance of nuclear lesions leading to apoptosis; (*ii*) increased detoxification of cisplatin by metallothionein and glutathione; and (*iii*) diminished accumulation of cisplatin (2, 6, 8). Of these mechanisms, accumulation defect seems to be dominant in various cell lines (8, 43). As mentioned above, CP-r cells have a defect in endocytosis (32), which may lead to diminished accumulation of cisplatin and confer the cells on resistance against extracellular cisplatin. The restored endocytosis of transferrin by $[Gd@C_{82}(OH)_{22}]_n$ nanoparticles indicated that the nanoparticles can circumvent the acquired resistance of the CP-r PC-3-luc variants by enhancing uptake of cisplatin (Fig. 5 and Movie S1). Cisplatin sensitivity was also increased by nanoparticles in CP-r KB-3–1 and BEL 7404 cells (Fig. S6). Because intracellular accumulation of cisplatin is reduced in CP-r cells due to a pleiotropic defect, other mechanisms such as reduced fluidity of plasma membrane or altered cytoskeleton may also contribute to the $[Gd@C_{82}(OH)_{22}]_n$ nanoparticle reversal of the cisplatin resistance in vitro and in vivo (9, 10). Bioeffect of nanoparticles was measured with LIVE/DEAD Viability/Cytotoxicity by using confocal microscopy (Fig. S7). These nanoparticles are surprisingly nontoxic to cancer cells in vitro, yet can successfully enhance the growth inhibition by cisplatin on CP-r tumor in vivo. The in vivo enhancing effect of the nanoparticles may also partially contribute to their penetration and accumulation in the leaky vasculature of tumors (44). In conclusion, using nanomaterials to overcome the drug resistance of malignant tumors could lead to new therapies for cancer patients. This provides a promising chemotherapeutic method to treat tumors at lower, nontoxic dose levels.

Materials and Methods

[Gd@C₈₂ (OH)₂₂]ₙ Nanoparticles. $Gd@C82$ was synthesized by the method of Krätschmer-Huffman (45) and extracted under high temperature and high pressure (46). A high performance liquid chromatography (LC908-C60, Japan Analytical Industry Co.) coupled with 5PBB and Buckyprep columns (Nacalai) was used to separate $Gd@C82$ from other metallofullerenes (47). The final purity of the $Gd@C82$ was greater than 99.5% as measured by MADLI-TOF-MS (Auto-Flex, Bruker). Hydroxylation was performed by alkaline reaction (47, 48). The $Gd@C82(OH)_x$ was isolated using Sephadex G-25 column chromatography (5×50 cm^2) with an eluent of neutralized water (47). A fraction of the eluate was collected over a short time interval to ensure that the hydroxyl number distribution was in a narrow range.

MRI. Athymic nude mice were anesthetized using 2% isoflurane, and the tumors were positioned at the center of the RF coil. The physiologic conditions of the animals were monitored using a respiratory monitoring device during the scanning. The animals were scanned using a Bruker 400 MHz, 89-mm NMR spectrometer. After a pilot scan for determining the region of interest, a multislice spin-echo sequence was used with repetition time (TR) of 2 s, echo time (TE) of 25 ms, and slice thickness of 1 mm. The tumor sizes were calculated using Image J software (National Institutes of Health).

Optical imaging. Luciferase was used as a marker in optical images to evaluate the growth of tumors by using the Xenogen IVIS Imaging System (Caliper Life Sciences). Anesthetized mice were i.p. injected with 75 mg/kg D-Luciferin (Caliper Life Sciences) in PBS. Eight minutes after injection, bioluminescence images were acquired using optical imaging. The acquisition time was 0.1 s. Images were set at the indicated pseudocolor scale to show relative bioluminescent changes over time.

Endocytosis of Texas Red–Transferrin. The CP-s and CP-r PC-3-luc cells were labeled with 10 μg/mL Texas Red–transferrin for 20 min at 37 °C. Texas Red-transferrin was removed by a PBS rinse. Cells labeled with Texas Red–transferrin were cultured in RPMI medium with 1 μg/mL cisplatin for 40 min, fixed by 70% ethanol in PBS, then imaged by spinning disk confocal microscope (Yokogawa). $[Gd@C_{82}(OH)_{22}]_n$ nanoparticles (20 μM) and cisplatin (1 μg/mL) were used in each individual experiment to measure the endocytosis of Texas Red–transferrin.

DNA Adducts Measured by Inductively Coupled Plasma Mass Spectroscopy. The CP-s and CP-r PC-3-luc cells were grown at a density of 10^5 cells/mL. Cells were exposed to 1 μg/mL cisplatin for 40 min with or without 20 μM $[Gd@C_{82}(OH)_{22}]$ n nanoparticles. Cells were trypsinized, washed with PBS, and centrifuged for 6 min at $1,000 \times g$. The DNA was then extracted and digested as reported in the previous studies (49, 50). The mass spectrometer used was a Thermo Biosystems $\times 7$ inductively coupled plasma mass spectroscopy (ICP-MS) instrument. Measurements were made in the negative ion mode with the source temperature.

Experimental Details. Experimental details on preparation of $[Gd@C_{82}(OH)_{22}]_n$ nanoparticles, establishment of the cisplatin-resistant cells, transferrin-mediated endocytosis, and cell proliferation assay are included in SI Text.

1. Gottlieb JA, Drewinko B (1975) Review of the current clinical status of platinum coordination complexes in cancer chemotherapy. *Cancer Chemother Rep* 59:621–628.
2. Wang D, Lippard SJ (2005) Cellular processing of platinum anticancer drugs. *Nat Rev Drug Discov* 4:307–320.
3. Borst P, Rottenberg S, Jonkers J (2008) How do real tumors become resistant to cisplatin? *Cell Cycle* 7:1353–1359.
4. Siddik ZH (2003) Cisplatin: Mode of cytotoxic action and molecular basis of resistance. *Oncogene* 22:7265–7279.
5. Kartner N, Riordan JR, Ling V (1983) Cell surface P-glycoprotein associated with multidrug resistance in mammalian cell lines. *Science* 221:1285–1288.
6. Kelland LR (2000) Preclinical perspectives on platinum resistance. *Drugs* 59(Suppl 4):1–8, discussion 37–38.
7. Liang XJ, Shen DW, Gottesman MM (2004) A pleiotropic defect reducing drug accumulation in cisplatin-resistant cells. *J Inorg Biochem* 98:1599–1606.
8. Ozols RF, O'Dwyer PJ, Hamilton TC, Young RC (1990) The role of glutathione in drug resistance. *Cancer Treat Rev* 17(Suppl A):45–50.
9. Hall MD, Okabe M, Shen DW, Liang XJ, Gottesman MM (2008) The role of cellular accumulation in determining sensitivity to platinum-based chemotherapy. *Annu Rev Pharmacol Toxicol* 48:495–535.
10. Liang XJ, Shen DW, Garfield S, Gottesman MM (2003) Mislocalization of membrane proteins associated with multidrug resistance in cisplatin-resistant cancer cell lines. *Cancer Res* 63:5909–5916.
11. Safaei R, et al. (2005) Intracellular localization and trafficking of fluorescein-labeled cisplatin in human ovarian carcinoma cells. *Clin Cancer Res* 11:756–767.

Liang et al.

MEDICAL SCIENCES

CHEMISTRY

12. Safaei R, et al. (2005) Abnormal lysosomal trafficking and enhanced exosomal export of cisplatin in drug-resistant human ovarian carcinoma cells. *Mol Cancer Ther* 4: 1595–1604.

13. McNeill DR, Wilson DM, 3rd (2007) A dominant-negative form of the major human abasic endonuclease enhances cellular sensitivity to laboratory and clinical DNA-damaging agents. *Mol Cancer Res* 5:61–70.

14. Basu S, et al. (2009) Nanoparticle-mediated targeting of MAPK signaling predisposes tumor to chemotherapy. *Proc Natl Acad Sci USA* 106:7957–7961.

15. Dhar S, Gu FX, Langer R, Farokhzad OC, Lippard SJ (2008) Targeted delivery of cisplatin to prostate cancer cells by aptamer functionalized Pt(IV) prodrug-PLGA-PEG nanoparticles. *Proc Natl Acad Sci USA* 105:17356–17361.

16. Hamelers IH, et al. (2009) High cytotoxicity of cisplatin nanocapsules in ovarian carcinoma cells depends on uptake by caveolae-mediated endocytosis. *Clin Cancer Res* 15:1259–1268.

17. Kroto HW, Heath JR, O'Brien SC, Curl RF, Smalley RE (1985) C60: Buckminsterfullerene. *Nature* 318:162–163.

18. Tabata Y, Murakami Y, Ikada Y (1997) Photodynamic effect of polyethylene glycol-modified fullerene on tumor. *Jpn J Cancer Res* 88:1108–1116.

19. Yin JJ, et al. (2009) The scavenging of reactive oxygen species and the potential for cell protection by functionalized fullerene materials. *Biomaterials* 30:611–621.

20. Yin JJ, et al. (2008) Inhibition of tumor growth by endohedral metallofullerenol nanoparticles optimized as reactive oxygen species scavenger. *Mol Pharmacol* 74: 1132–1140.

21. Wang JX, et al. (2006) Antioxidative function and biodistribution of [Gd@C82(OH)22]n nanoparticles in tumor-bearing mice. *Biochem Pharmacol* 71:872–881.

22. Chen CY, et al. (2005) Multihydroxylated [Gd@C82(OH)22]n nanoparticles: Antineoplastic activity of high efficiency and low toxicity. *Nano Lett* 5:2050–2057.

23. MacFarland DK, et al. (2008) Hydrochalarones: A novel endohedral metallofullerene platform for enhancing magnetic resonance imaging contrast. *J Med Chem* 51: 3681–3683.

24. Xing GM, et al. (2008) The strong MRI relaxivity of paramagnetic nanoparticles. *J Phys Chem B* 112:6288–6291.

25. Bolskar RD, et al. (2003) First soluble M@C60 derivatives provide enhanced access to metallofullerenes and permit in vivo evaluation of Gd@C60[C(COOH)2]10 as a MRI contrast agent. *J Am Chem Soc* 125:5471–5478.

26. Kato H, et al. (2003) Lanthanoid endohedral metallofullerenols for MRI contrast agents. *J Am Chem Soc* 125:4391–4397.

27. Laus S, et al. (2005) Destroying gadofullerene aggregates by salt addition in aqueous solution of Gd@C(60)(OH)(x) and Gd@C(60)[C(COOH(2))](10). *J Am Chem Soc* 127: 9368–9369.

28. Tang J, et al. (2006) Periodical variation of electronic properties in polyhydroxylated metallofullerene materials. *Adv Mater* 18:1458–1462.

29. Jiang W, Kim BY, Rutka JT, Chan WC (2008) Nanoparticle-mediated cellular response is size-dependent. *Nat Nanotechnol* 3:145–150.

30. Liang XJ, Chen C, Zhao Y, Jia L, Wang PC (2008) Biopharmaceutics and therapeutic potential of engineered nanomaterials. *Curr Drug Metab* 9:697–709.

31. Da Ros T, Prato M (1999) Medicinal chemistry with fullerenes and fullerene derivatives. *Chem Commun (Camb)* 8:663–669.

32. Liang XJ, Mukherjee S, Shen DW, Maxfield FR, Gottesman MM (2006) Endocytic recycling compartments altered in cisplatin-resistant cancer cells. *Cancer Res* 66: 2346–2353.

33. Kawai K, Kamatani N, Georges E, Ling V (1990) Identification of a membrane glycoprotein overexpressed in murine lymphoma sublines resistant to cis-diamminedichloroplatinum(II). *J Biol Chem* 265:13137–13142.

34. Shen DW, Akiyama S, Schoenlein P, Pastan I, Gottesman MM (1995) Characterisation of high-level cisplatin-resistant cell lines established from a human hepatoma cell line and human KB adenocarcinoma cells: Cross-resistance and protein changes. *Br J Cancer* 71:676–683.

35. Shen DW, Liang XJ, Gawinowicz MA, Gottesman MM (2004) Identification of cytoskeletal [14C]carboplatin-binding proteins reveals reduced expression and disorganization of actin and filamin in cisplatin-resistant cell lines. *Mol Pharmacol* 66: 789–793.

36. Chauhan SS, et al. (2003) Reduced endocytosis and altered lysosome function in cisplatin-resistant cell lines. *Br J Cancer* 88:1327–1334.

37. Liang XJ, et al. (2005) Trafficking and localization of platinum complexes in cisplatin-resistant cell lines monitored by fluorescence-labeled platinum. *J Cell Physiol* 202: 635–641.

38. Shen DW, Su A, Liang XJ, Pai-Panandiker A, Gottesman MM (2004) Reduced expression of small GTPases and hypermethylation of the folate binding protein gene in cisplatin-resistant cells. *Br J Cancer* 91:270–276.

39. Ambrose KR, Lowrey JS (1982) Effect of cis- and trans-dichlorodiammineplatinum(II) on human tumor cell proliferation in diffusion chambers in vivo. *Cancer Res* 42: 1769–1773.

40. Gately DP, Howell SB (1993) Cellular accumulation of the anticancer agent cisplatin: A review. *Br J Cancer* 67:1171–1176.

41. Sharp SY, Rogers PM, Kelland LR (1995) Transport of cisplatin and bis-acetato-ammine-dichlorocyclohexylamine Platinum(IV) (JM216) in human ovarian carcinoma cell lines: Identification of a plasma membrane protein associated with cisplatin resistance. *Clin Cancer Res* 1:981–989.

42. Larson CA, Blair BG, Safaei R, Howell SB (2009) The role of the mammalian copper transporter 1 in the cellular accumulation of platinum-based drugs. *Mol Pharmacol* 75:324–330.

43. Andrews PA, Howell SB (1990) Cellular pharmacology of cisplatin: Perspectives on mechanisms of acquired resistance. *Cancer Cells* 2:35–43.

44. Murphy EA, et al. (2008) Nanoparticle-mediated drug delivery to tumor vasculature suppresses metastasis. *Proc Natl Acad Sci USA* 105:9343–9348.

45. Kratschmer W, Lamb LD, Fostiropoulos K, Huffman DR (1990) Solid C60: A new form of carbon. *Nature* 347:354–358.

46. Sun B, Feng L, Shi Z, Gu Z (2002) Improved extraction of metallofullerenes with DMF at high temperature. *Carbon* 40:1591–1595.

47. Xing G, et al. (2004) Influences of structural properties on stability of fullerenols. *J Phys Chem B* 108:11473–11479.

48. Mikawa M, et al. (2001) Paramagnetic water-soluble metallofullerenes having the highest relaxivity for MRI contrast agents. *Bioconjug Chem* 12:510–514.

49. Box HC, et al. (2002) Detection and characterization of formamido lesions in DNA by liquid chromatography-mass spectrometry. *Radiat Res* 158:538–542.

50. Dawidzik JB, et al. (2003) DNA damage measured by liquid chromatography-mass spectrometry in mouse fibroblast cells exposed to oxidative stress. *Biochim Biophys Acta* 1621:211–217.

www.manaraa.com